Eur. Phys. J. A **15**, 351–356 (2002)
DOI 10.1140/epja/i2002-10034-8

THE EUROPEAN PHYSICAL JOURNAL A

Transfer reactions and sub-barrier fusion in ^{40}Ca + ^{90,96}Zr

G. Montagnoli[1,a], S. Beghini[1], F. Scarlassara[1], A.M. Stefanini[2], L. Corradi[2], C.J. Lin[2,b], G. Pollarolo[3], and Aage Winther[4]

[1] Dipartimento di Fisica, Universitá di Padova, and Istituto Nazionale di Fisica Nucleare, Sezione di Padova, via Marzolo 8, I-35131, Padova, Italy
[2] Istituto Nazionale di Fisica Nucleare, Laboratori Nazionali di Legnaro, I-35020 Legnaro, Padova, Italy
[3] Dipartimento di Fisica Teorica, Universitá di Torino, and Istituto Nazionale di Fisica Nucleare, Sezione di Torino, I-10125 Torino, Italy
[4] The Niels Bohr Institute, Blegdamsvej 17, DK-2100 Copenhagen Ø, Denmark

Received: 2 May 2002 / Revised version: 4 June 2002 /
Published online: 26 November 2002 –
Communicated by C. Signorini

Abstract. The two systems ^{40}Ca + ^{90,96}Zr have been studied by measuring nucleon transfer reactions at two energies near the Coulomb barrier, thus complementing the available sub-barrier fusion cross-sections. Angular distributions for various transfer channels have been determined. Significantly larger neutron transfer cross-sections are found for the target ^{96}Zr that exhibits the larger enhancement in the sub-barrier fusion cross-sections. All data have been analyzed with a new model for heavy-ion collisions that calculates simultaneously transfer cross-sections, fusion excitation functions and barrier distributions. The model gives a good account of both transfer and fusion data.

PACS. 25.70.Hi Transfer reactions – 25.70.Jj Fusion and fusion-fission reactions – 24.10.-i Nuclear-reaction models and methods

1 Introduction

The dynamics of heavy-ion reactions at energies close to the Coulomb barrier is intimately linked to the structure of the two colliding nuclei. That link shows up dramatically in the strong enhancements of sub-barrier fusion cross-sections. These display large isotopic variations that have been related to the properties (energy, multipolarity and strength) of the low-lying surface vibrational modes and possibly to the transfer of neutrons [1,2].

In recent years, the development of high-resolution and efficient experimental set-ups (see, *e.g.*, [3]) has allowed detailed studies of transfer reactions in the energy range near the Coulomb barrier [4–11], for various combinations of targets and projectiles. However, in spite of a long-standing debate [12–15], the relevance of transfer channels to sub-barrier fusion is not yet clarified. This is partly due to the difficulty of treating, within a single formalism, the full body of reactions that take place in a collision between heavy ions.

A recent attempt to overcome these difficulties was carried out by Esbensen *et al.* [16] by a coupled-channels (CC) analysis of fusion excitation function, inelastic and transfer cross-sections in the ^{58}Ni + ^{124}Sn system [8]. They used a CC code that incorporates the incoming-wave boundary condition and uses the rotating-frame approximation in order to reduce the number of neutron transfer couplings. This approximation, quite good at energies below the Coulomb barrier, may be somewhat limiting at higher energies when the transfer of angular momentum starts to play a role. As we will discuss below, the angular-momentum transfer is very important in defining the energy dependence of the barrier distributions. Low-lying surface modes of target and projectile, all single-neutron transfer and (by successive approximations) multi-neutron transfer channels were included in the CC calculations of ref. [16]. Charged-particle transfer was simulated by an imaginary potential, and a very good description of the measured quasi-elastic, fusion and transfer cross-sections was obtained.

The main conclusion of ref. [16] was that transfer channels do enhance sub-barrier fusion cross-sections for ^{58}Ni + ^{124}Sn, but the enhancement is not as strong as the effect of coupling to low-lying surface modes. However, the limited accuracy and the large energy step of the measurements did not allow extracting a fusion barrier distribution

[a] e-mail: montagnoli@pd.infn.it, Fax +39049 8277102, Tel. +39049 8277117.
[b] On leave from the China Institute for Atomic Energy, 102413 Beijing, China.

as the second energy-weighted derivative of the excitation function [17], and no data were available for a comparison with nearby systems.

The pair of systems ^{40}Ca + ^{90,96}Zr constitute an ideal case since detailed fusion excitation functions were measured [18] showing a conspicuous isotopic effect, and the two barrier distributions are quite different from each other. The larger sub-barrier enhancement of ^{40}Ca + ^{96}Zr and its broader and structureless barrier distribution were attributed to the strong influence of neutron transfer channels. Actually, CC calculations that included the collective excitations of the colliding nuclei only, strongly underpredicted [18] the sub-barrier fusion yield for ^{40}Ca + ^{96}Zr and did not reproduce the shape of its barrier distribution.

A semi-classical theory [19–21] has been developed in the past few years, that, starting from the structure of the two colliding nuclei, calculates fusion, quasi-elastic and transfer cross-sections at the same time. This theory has been successfully used to analyze a variety of multinucleon transfer reactions [9–11]; it is able to reproduce the main features of such reactions quite well, as far as mass, charge, angular distributions and Q-value spectra are concerned. More recently the same calculations have been extended to sub-barrier fusion cross-sections and barrier distributions [22].

Therefore, we have performed the experimental study of quasi-elastic and transfer reactions in ^{40}Ca + ^{90,96}Zr near the Coulomb barrier. This paper presents the outcome of such experiments and the data analysis performed with the GRAZING model [19] of the transfer results and of the high-quality fusion data, trying to understand the interplay between surface and nucleon transfer degrees of freedom in the tunneling process. A preliminary account of the transfer experiments, with no theoretical interpretation, was presented in ref. [23].

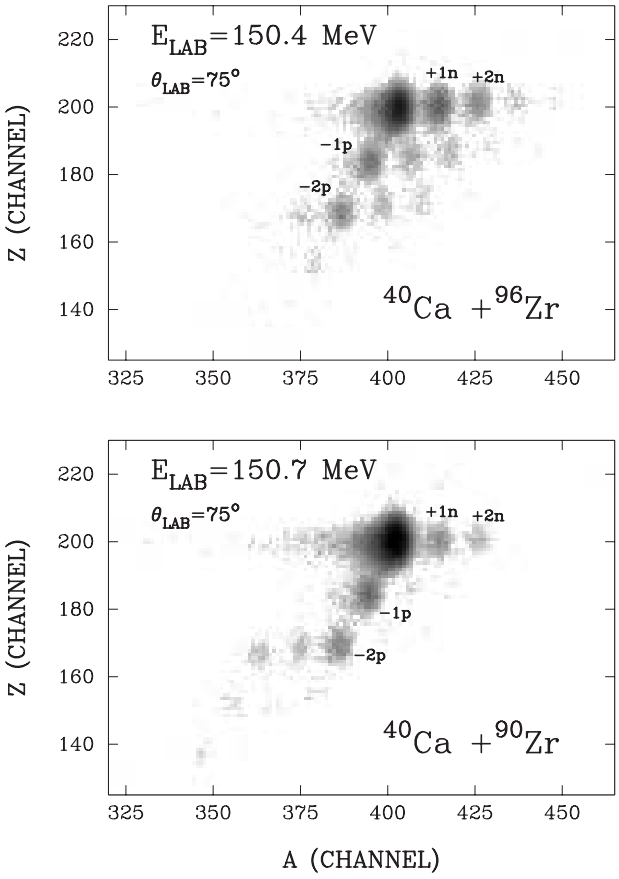

Fig. 1. Two-dimensional plots Z *vs.* mass number A of the beam-like fragments at $E_{\rm lab} = 152$ MeV; the reported energies are the beam energies at half of the target thickness. Events belonging to a certain mass, but to different Z-numbers, do not fall exactly on a vertical line due to small data analysis offsets.

2 The experiments

The experiments were performed using the ^{40}Ca beam (5–10 pnA) of the XTU Tandem accelerator of the Laboratori Nazionali di Legnaro. The transfer reactions were studied at $E_{\rm lab} = 152$ MeV for both targets and 135.5 MeV for ^{96}Zr only. The lower energy is 4 MeV below the nominal Coulomb barrier ($\simeq$ 139.3 MeV). The zirconium oxide targets had thicknesses 150(200) μg/cm^2, and were evaporated on 45(30)μg/cm^2 carbon foils, with isotopic enrichments 99.36% and 95.63% for ^{90}Zr and ^{96}Zr, respectively. The same target material was used in the previous fusion experiment [18]. The "effective" beam energies, at half of the target thickness, were 150.4 and 133.8 MeV for ^{96}Zr and 150.7 MeV for ^{90}Zr.

Projectile-like reaction fragments were detected by PISOLO which is a time-of-flight (TOF) spectrometer with magnetic focusing, start- and stop-detectors based on micro-channel plates, and with a split-anode ionization chamber for $\Delta E/E$ measurements; more details about PISOLO can be found in [3]. The mass A and nuclear charge Z resolutions ($\simeq 1/100$ and $\simeq 1/60$, respectively) allowed unambiguous identification of the reaction products. This can be appreciated from fig. 1 that shows two-dimensional Z *vs.* A spectra for the two systems at the higher energy, measured at $\theta_{\rm lab} = 75°$ (near the grazing angle). The two spectra are remarkably different: for ^{40}Ca + ^{90}Zr most of the transfer cross-section is concentrated in one- and two-neutron pick-up channels and in one- and two-proton stripping channels. For ^{40}Ca + ^{96}Zr a significant population of the +3n, +4n and −3p channels, and of all mixed neutron-proton transfer channels is observed. It is worth noticing that in the ^{90}Zr case the stripping channel $-2p-2n$ (or of an α-cluster) is relatively strong.

Angular distributions were measured in the range $40° \leq \theta_{\rm lab} \leq 105°$ at 152 MeV, and in the range $65° \leq \theta_{\rm lab} \leq 120°$ at the lower energy. Figure 2 shows, for the indicated energies, the angular distributions of one- and two-neutron pick-up and of one- and two-proton stripping, which are the most relevant channels observed for both Zr targets. Comparing the two higher energies, the neutron pick-up cross-sections of ^{40}Ca + ^{96}Zr are almost a factor ten larger than the corresponding ones in the ^{40}Ca + ^{90}Zr. On the contrary, proton stripping channels have compa-

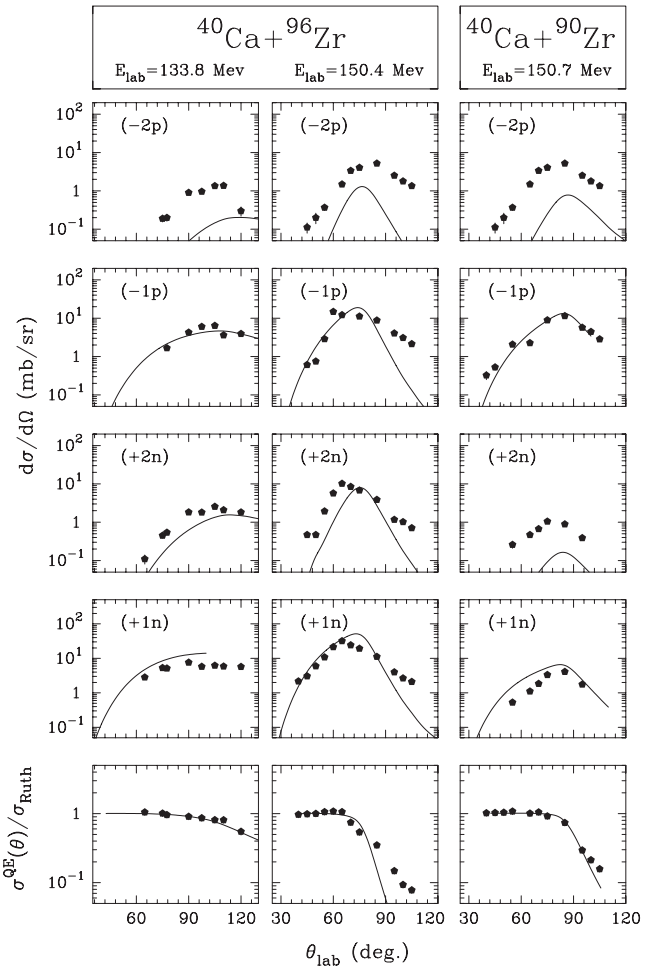

Fig. 2. Angular distributions for one- and two-particle transfer (integrated over the Q-value distributions) in ^{40}Ca + ^{90,96}Zr at the indicated energies. Dots are experimental values, lines are the results of GRAZING calculations (see text). The lowest panels show the elastic plus inelastic cross-sections (normalized to the Rutherford values).

rable cross-sections in the two systems. Angular distributions were already shown in ref. [23] even for more complex transfer channels; there, one can also find representative cases of Q-value distributions.

Quasi-elastic angular distributions have also been measured for both systems, and they are shown in the lowest panels of fig. 2.

3 Data analysis

The data have been analyzed with the GRAZING model [19–21], which calculates, at the same time, the redistribution of mass and charge between the two ions (few- and multi-nucleon transfer), quasi-elastic and fusion cross-sections. We start the discussion from fusion which is actually the larger part of the total reaction cross-section near and above the Coulomb barrier and its correct evaluation is essential for giving reliable estimates for the transfer yields. Following ref. [22] the fusion cross-section at the center-of-mass energy E is calculated as

$$\sigma(E) = \sum_{\ell} \frac{\pi\hbar^2}{2m_{aA}E}(2\ell+1)T_\ell(E)\,, \tag{1}$$

where $T_\ell(E)$ is the transmission probability through the potential barrier for the partial wave ℓ, and m_{aA} is the reduced mass of the system. Using the inverse parabolic approximation the transmission coefficient becomes

$$T_\ell(E) = \frac{1}{1+\exp[2\pi(E_{\rm b}-E)/\hbar\omega_{\rm b}]}\,, \tag{2}$$

where $E_{\rm b}$ is the barrier of the effective potential $U_{\rm eff}$ and $\omega_{\rm b}$ is the frequency of the relative motion

$$\omega_{\rm b} = \sqrt{\frac{1}{m_{aA}}\frac{\partial^2 U_{\rm eff}}{\partial r^2}}. \tag{3}$$

Due to the coupling between the relative motion and the intrinsic degrees of freedom (surface modes and exchange of nucleons), the system, in its approaching phase, sees a distribution of barriers. Therefore, the true transmission coefficient is obtained by folding $T_\ell(E)$ with the barrier distribution $P(E_r)$, *i.e.*

$$T_\ell(E) = \int_{-\infty}^{+\infty} P(E_r)T_\ell(E-E_r){\rm d}E_r\,. \tag{4}$$

It is clear from the above expression that, contrary to other models, in order to calculate the fusion cross-section one must first calculate the barrier distribution. Its shape is energy dependent and is determined by the dynamics of the reaction. This energy dependence is very weak below the Coulomb barrier, and the distribution becomes wider and bell-shaped at higher energies essentially due to the transfer of angular momentum (for more details see ref. [22]).

The relative motion of the two ions is determined by the simple parameterization of ref. [24] for the nuclear potential, obtained from a best fit analysis over several elastic-scattering angular distributions. It is not a surprise that small adjustments of the potential parameters may still be needed from case to case. To this end, the model allows to modify the radius of the nuclear potential introducing a shift ΔR.

Since tunneling probabilities are influenced by the motion of the two nuclear surfaces, a modification of the reduced mass appearing in eq. (3) was performed in refs. [20, 22]. This was done by exploiting the fact that, for pure nuclear interaction, the form factors for the excitation of the surface modes have the same radial shape as the force acting on the relative motion variable. On the other hand, in actual cases one cannot neglect the Coulomb interaction (here the form factors and the force acting on the relative motion variable do not have the same radial shape); hence we have multiplied the modified reduced mass (see [20, 22]) by a scaling factor $\delta_{\rm s}$ which takes into account the Coulomb interaction.

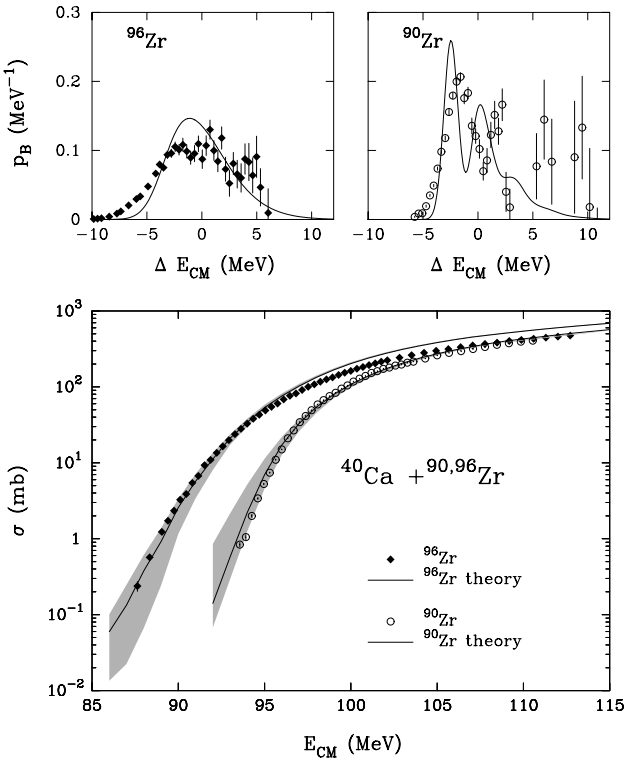

Fig. 3. Fusion excitation functions (lower panel) and barrier distributions for ^{40}Ca + ^{90,96}Zr, as reported in [21]; the lines are the results of the calculations described in the text. In the upper panels, the energy scale is relative to the nominal Coulomb barriers.

By including the low-lying 2^+ and 3^- states of projectile and target [25] and treating the transfer channels in the independent particle picture, one obtains, for each energy, a fusion barrier distribution which is then used to calculate the corresponding fusion cross-section. Examples of these distributions, for energies lower than the nominal Coulomb barriers, are shown in the upper part of fig. 3 and compared with the "experimental" barrier distributions obtained as the second energy-weighted derivatives of the excitation functions (this comparison can be only qualitative, since different quantities are actually plotted together). The corresponding calculated fusion excitation functions are reported in the lower panel of fig. 3 (full lines).

All these results have been obtained by using the following set of parameters derived from the systematics of ref. [22]: $\Delta R = -0.02$ fm and $\delta_s = 0.8$ for ^{40}Ca + ^{96}Zr and $\Delta R = -0.15$ fm and $\delta_s = 0.1$ for ^{40}Ca + ^{90}Zr. The gray regions indicate the sensitivity of our calculations to the parameter δ_s, where the lowest cross-sections are obtained by neglecting the effect of the surface motion on the tunneling probabilities ($\delta_s = 0.0$), while the highest ones are calculated by including the correction with pure nuclear interaction ($\delta_s = 1.0$). The isotopic dependence of the fusion excitation function is well reproduced by the model, irrespective of the chosen value for δ_s.

The different shapes of the two barrier distributions are correctly calculated, even if fusion cross-sections of ^{40}Ca + ^{96}Zr are overpredicted above the barrier by 30%. We stress, anyway, that the experimental accuracy of the absolute cross-section scale for each system is ±15% [13]. Relative errors within each system are essentially only statistical ones; going from ^{40}Ca + ^{90}Zr to ^{40}Ca + ^{96}Zr the relative cross-section scale is determined by uncertainties in the angular distribution measurements and integration ($\simeq 7\%$) and by possible differences ($\simeq 5\%$) in the set-up transmission for the two systems (see [13] and refs. therein for more details).

A detailed analysis of the calculated contributions from the various inelastic channels [22] leads to the conclusion that the peakless shape observed for the barrier distribution of ^{40}Ca + ^{96}Zr is essentially due to the strength of the octupole vibration in ^{96}Zr, which is more collective and lies lower in energy than in ^{90}Zr. In the recent study of sub-barrier fusion for ^{36}S + ^{90,96}Zr [26], the comparison with ^{40}Ca + ^{90,96}Zr points to the same direction.

Indeed, the calculated contributions of the various couplings to the enhancements of the fusion cross-sections are shown in fig. 4. We see that for both systems the largest effect comes from inelastic excitations of low-lying states of projectile and target, in particular, from the octupole vibration in ^{40}Ca. We remember that these calculations give only a qualitative picture of the relative importance of the various couplings, since the form factor defining the coupling to each specific channel is strongly affected by the presence of the inelastic surface modes (it depends on the relative distance between the two nuclear surfaces).

The redistribution of mass and charge between projectile and target are calculated by using an independent particle description and by including all possible one-particle transfer couplings (stripping and pick-up of neutrons and protons). The simple analytical parameterization of ref. [27] is employed for the single-particle form factors and all open channels are counted by using an average single-particle level density (for more details see ref. [20]). The estimated cross-sections for multi-nucleon transfer channels are thus calculated in the sequential approximation. Figure 2 shows the calculations of the angular distributions of the indicated transfer channels in comparison with the present experimental results. The theory gives an overall good account of the data, in particular of the inclusive one-neutron pick-up and of the one-proton stripping reactions for both zirconium targets. The energy dependence is also quite well described for ^{96}Zr. Two neutron pick-up cross-sections are reasonably well reproduced, while the model underestimates the two-proton stripping yields, as well as the multinucleon transfer channels (not shown in fig. 2) observed for ^{40}Ca + ^{96}Zr. Calculated Q-value distributions are narrower than experimental spectra, just as observed in our previous study of ^{64}Ni + ^{238}U [11].

In the bottom row of the same figure we display also the measured quasi-elastic cross-sections compared with the calculations. The comparison is good for ^{40}Ca + ^{90}Zr and for the lower energy of ^{40}Ca + ^{96}Zr. For ^{40}Ca + ^{96}Zr

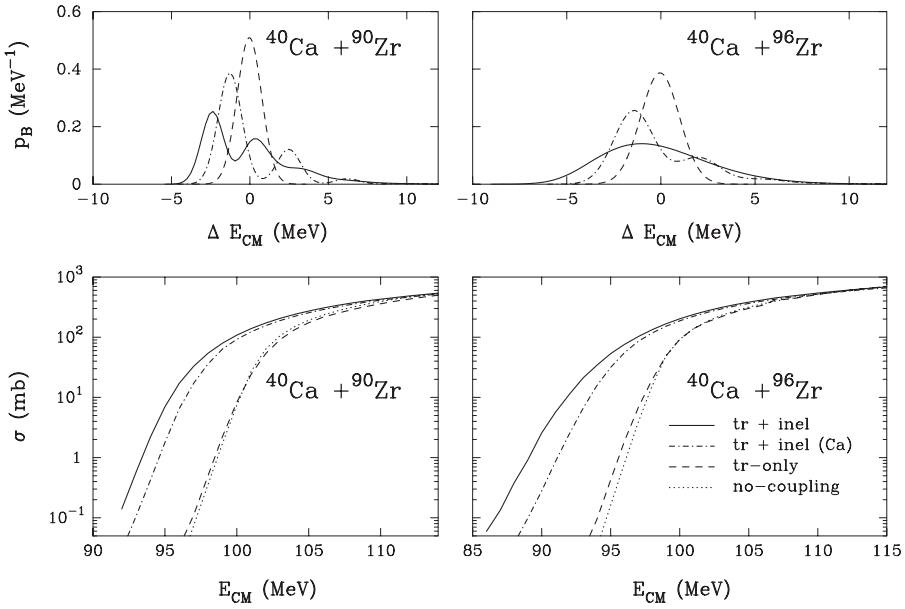

Fig. 4. GRAZING calculations of fusion for ^{40}Ca + ^{90,96}Zr, where the contributions of various channels are evidenced.

at the higher energy, the agreement between data and calculations is good at the level of the quarter-point angle. Hence, we are confident in the choice of the empirical potential used in the calculations, where the parameters were obtained from the systematics of ref. [24].

4 Summary

We have presented here the results of measurements of nucleon transfer reactions in ^{40}Ca + ^{90,96}Zr at two bombarding energies near the Coulomb barrier, performed by the TOF spectrometer PISOLO. Neutron pick-up cross-sections are much larger for ^{40}Ca + ^{96}Zr with respect to ^{40}Ca + ^{90}Zr, while proton stripping channels have comparable cross-sections in the two systems. The transfer data and the previously measured fusion excitation functions have been analyzed within the same semi-classical theory of refs. [19,20]. The model reproduces the main trends of the transfer data (in particular the larger transfer cross-sections observed for ^{40}Ca + ^{96}Zr) and, at the same time, gives a good account of the fusion excitation functions and of the barrier distributions.

The GRAZING model indicates: 1) a large influence of the inelastic excitations on the strong isotopic effect of fusion at sub-barrier energies, and in particular on the shape of the barrier distributions; 2) a less significant effect of transfer couplings on fusion, in agreement with the conclusions of the analysis performed by Esbensen *et al.* [16] for ^{58}Ni + ^{124}Sn.

We wish to acknowledge the professional work of the Tandem accelerator staff at LNL. In particular, we are grateful to F. Scarpa and to Mr. G. Binelle for the preparation of the good-quality ^{40}Ca beams.

References

1. A.B. Balantekin, N. Takigawa, Rev. Mod. Phys. **70**, 77 (1998).
2. M. Dasgupta, D.J. Hinde, N. Rowley, A.M. Stefanini, Annu. Rev. Nucl. Part. Sci. **48**, 401 (1998).
3. G. Montagnoli, F. Scarlassara, S. Beghini, A. Dal Bello, G.F. Segato, A.M. Stefanini, D. Ackermann, L. Corradi, J.H. He, C.J. Lin, Nucl. Instrum. Methods Phys. Res. A **454**, 306 (2000).
4. W. Von Oertzen, H.G. Bohlen, B. Gebauer, R. Künkel, F. Pühlhofer, D. Schüll, Z. Phys. A **326**, 463 (1987).
5. R. Künkel, W. Von Oertzen, B. Gebauer, H.A. Bösser, B. Kohlmeyer, F. Pühlhofer, D. Schüll, Phys. Lett. B **208**, 355 (1988).
6. J. Speer, W. Von Oertzen, D. Schüll, M. Wilpert, H.G. Bohlen, B. Gebauer, B. Kohlmeyer, F. Pühlhofer, Phys. Lett. B **259**, 422 (1991).
7. C.L. Jiang, K.E. Rehm, J. Gehring, B. Glagola, W. Kutschera, M. Rhein, A.H. Wuosmaa, Phys. Lett. B **337**, 59 (1994).
8. C.L. Jiang, K.E. Rehm, H. Esbensen, D.J. Blumenthal, B. Crowell, J. Gehring, B. Glagola, J.P. Schiffer, A.H. Wuosmaa, Phys. Rev. C **57**, 2393 (1998).
9. L. Corradi, J.H. He, D. Ackermann, A.M. Stefanini, A. Pisent, S. Beghini, G. Montagnoli, F. Scarlassara, G.F. Segato, G. Pollarolo, C.H. Dasso, A. Winther, Phys. Rev. C **54**, 201 (1996).
10. L. Corradi, A.M. Stefanini, J.H. He, C. Lin, S. Beghini, G. Montagnoli, F. Scarlassara, G.F. Segato, G. Pollarolo, C.H. Dasso, A. Winther, Phys. Rev. C **56**, 938 (1997).
11. L. Corradi, A.M. Stefanini, C. Lin, S. Beghini, G. Montagnoli, F. Scarlassara, G. Pollarolo, A. Winther, Phys. Rev. C **59**, 261 (1999).
12. C.R. Morton, M. Dasgupta, D.J. Hinde, J.R. Leigh, R.C. Lemmon, J.P. Lestone, J.C. Mein, J.O. Newton, H. Timmers, N. Rowley, A.T. Kruppa, Phys. Rev. Lett. **72**, 4074 (1994).

13. A.M. Stefanini, D. Ackermann, L. Corradi, J.H. He, G. Montagnoli, S. Beghini, F. Scarlassara, G.F. Segato, Phys. Rev. C **52**, R1727 (1995).
14. A.A. Sonzogni, J.D. Bierman, M.P. Kelly, J.P. Lestone, J.F. Liang, R. Vandenbosch, Phys. Rev. C **57**, 722 (1998).
15. H. Esbensen, S. Landowne, Nucl. Phys. A **492**, 473 (1989).
16. H. Esbensen, C.L.Jiang, K.E. Rehm, Phys. Rev. C **57**, 2401 (1998).
17. N. Rowley, G.R. Satchler, P.H. Stelson, Phys. Lett. B **254**, 25 (1991).
18. H. Timmers, D. Ackermann, S. Beghini, L. Corradi, J.H. He, G. Montagnoli, F. Scarlassara, A.M. Stefanini, N. Rowley, Nucl. Phys. A **633**, 421 (1998).
19. A. Winther, Nucl. Phys. A **572**, 191 (1994).
20. A. Winther, Nucl. Phys. A **594**, 203 (1995).
21. A. Winther, GRAZING, Computer code, unpublished (can be retrieved from `http://www.to.infn.it/~nanni/grazing`).
22. G. Pollarolo, A. Winther, Phys. Rev. C **62**, 054611 (2000).
23. G. Montagnoli, S. Beghini, F. Scarlassara, G.F. Segato, L. Corradi, C.J. Lin, A.M. Stefanini J. Phys. G.: Nucl. Part. Phys. **23**, 1431 (1997).
24. R. Broglia, A. Winther, *Heavy Ion Reactions* (Addison-Wesley, Redwood City CA, 1991).
25. M.R. Bhat, Nucl. Data Sheets **82**, 547 (1997).
26. A.M. Stefanini, L. Corradi, A.M. Vinodkumar, Yang Feng, F. Scarlassara, G. Montagnoli, S. Beghini, M. Bisogno, Phys. Rev. C **62**, 014601 (2000).
27. J.M. Quesada, G. Pollarolo, R.A. Broglia, A. Winther, Nucl. Phys. A **442**, 381 (1985).